Current Developments in Photocatalysis and Photocatalytic Materials

New Horizons in Photocatalysis

Edited by
Xinchen Wang, Masakazu Anpo
and Xianzhi Fu

ELSEVIER

Current Developments in Photocatalysis and Photocatalytic Materials

This page intentionally left blank

Current Developments in Photocatalysis and Photocatalytic Materials

New Horizons in Photocatalysis

Edited by

Xinchen Wang

Dean of the College of Chemistry and Director of the State Key Laboratory of Photocatalysis on Energy and Environment, Fuzhou University, Fuzhou, P. R. China

Masakazu Anpo

Special Honor Professor and International Advisor, State Key Laboratory of Photocatalysis on Energy and Environment, Fuzhou University, Fuzhou, P. R. China; Emeritus Professor, Osaka Prefecture University, Osaka, Japan

Xianzhi Fu

President, Fuzhou University, Fuzhou, P. R. China

ELSEVIER

Elsevier
Radarweg 29, PO Box 211, 1000 AE Amsterdam, Netherlands
The Boulevard, Langford Lane, Kidlington, Oxford OX5 1GB, United Kingdom
50 Hampshire Street, 5th Floor, Cambridge, MA 02139, United States

Notices
Knowledge and best practice in this field are constantly changing. As new research and experience broaden our understanding, changes in research methods, professional practices, or medical treatment may become necessary.

Practitioners and researchers must always rely on their own experience and knowledge in evaluating and using any information, methods, compounds, or experiments described herein. In using such information or methods they should be mindful of their own safety and the safety of others, including parties for whom they have a professional responsibility.

To the fullest extent of the law, neither the Publisher nor the authors, contributors, or editors, assume any liability for any injury and/or damage to persons or property as a matter of products liability, negligence or otherwise, or from any use or operation of any methods, products, instructions, or ideas contained in the material herein.

Library of Congress Cataloging-in-Publication Data
A catalog record for this book is available from the Library of Congress

British Library Cataloguing-in-Publication Data
A catalogue record for this book is available from the British Library

ISBN: 978-0-12-819000-5

Publisher: Susan Dennis
Acquisition Editor: Anneka Hess
Editorial Project Manager: Ruby Smith
Production Project Manager: Vignesh Tamil
Cover Designer: Christian Bilbow

Typeset by TNQ Technologies

Contents

Chapter 13: Seizing solar hydrogen from water promoted by magic spin transporting, chiral-induced spin state—selective filtering and upconversion

Wenyan Zhang[1] Gongxuan Lu[2]

[1]College of Material Engineering, Jinling Institute of Technology, Nanjing, China; [2]State Key Laboratory for Oxo Synthesis and Selective Oxidation, Lanzhou Institute of Chemical Physics, Chinese Academy of Sciences, Lanzhou, China

Chapter 14: Recent advances in the development of photocatalytic NOx abatement

Van-Huy Nguyen[1] Joseph Che-Chin Yu[2] Chao-Wei Huang[3] Jeffrey C.-S. Wu[2]

[1]Institute of Research and Development, Duy Tan University, Da Nang, Vietnam; [2]Department of Chemical Engineering, National Taiwan University, Taipei, Taiwan; [3]Department of Chemical and Materials Engineering, National Kaohsiung University of Science and Technology, Kaohsiung, Taiwan

About the editors

Professor Xinchen Wang is currently the director of the State Key Laboratory of Photocatalysis on Energy and Environment and the dean of college of chemistry in Fuzhou University. He obtained his BSc and MSc in Fuzhou University and went to The Chinese University of Hong Kong to pursue his PhD. In 2006, he moved to Tokyo University as a JSPS postdoctor, and then he went to Max Planck Institute of Colloide and Interfaces, Germany, as Alexander von Humboldt fellow, and was promoted as a Group Leader during 2008−2012. He started his professorship in Fuzhou University at 2005. His research interests cover catalysis and photocatalysis, and in this research field, he published more than 200 peer-reviewed papers with H-index of 96.

Professor Masakazu Anpo is presently a Special Honor Professor and International Advisor of the State Key Laboratory of Photocatalysis on Energy and Environment, Fuzhou University. He worked for 40 years at Osaka Prefecture University and served as Dean, Vice President, and Executive Director for last 10 years and is now a Professor Emeritus. He is a pioneer in the research of photochemical reactions on solid surfaces, design of visible light−responsive TiO_2 photocatalysts, and single-site heterogeneous photocatalysts constructed within zeolites. He is the editor-in-chief of *Res. Chem. Intermed*. (Springer). He has published more than 100 books and 500 original peer-reviewed papers. He is a member of Academia Europaea and Science Council of Japan.

Professor Xianzhi Fu received his PhD degree in Physical Chemistry from Peking University, China, in 1991. He did postdoctoral research on catalysis and photocatalysis at Peking University and University of Wisconsin-Madison, respectively. He joined Fuzhou University in 1997 where he was promoted to a full professor in 1998. Currently, he is the President of Fuzhou University. His research interests are mainly focused on Photocatalysis. He is the author or coauthor of more than 300 peer-reviewed scientific publications and 40 patents. Professor Fu has won many important awards including the National Science and Technology Progress Award. He was elected as a member of the Chinese Academy of Engineering in 2009.

This page intentionally left blank

Preface

It can be said that we are now facing serious and urgent issues regarding the lack of natural energy resources and fossil fuel–driven pollution and environmental degradation on a global scale. The increase in world population and rampant unregulated industrial growth have all led to accelerated energy consumption and the unabated release of toxic agents and industrial wastes into the air and waterways, leading to pollution-related disease and abnormal climate change such as global warming. In addition, the earthquake–tsunami disaster of March 11, 2011, which destroyed the reactors of the nuclear power plants in Fukushima, Japan, has raised serious concerns over the supply of electric power which seemed to reduce dependency on fossil fuels but, in fact, requires coolants polluted with radioactive materials and creates highly radioactive nuclear waste as a by-product.

It is, thus, vital to realize and construct novel energy production and conversion systems that utilize natural renewable energy and allow sustainable development without environmental deterioration. The decomposition of H_2O into H_2 and O_2 using visible light–responsive photocatalysts under sunlight irradiation has been intensively investigated as one of the most promising environmentally benign energy production systems to address these issues. In the past half century, research on various photocatalytic systems using mainly inorganic semiconducting materials such as TiO_2 metal oxides have been carried out. However, to achieve higher efficiency in the production of H_2, more innovative breakthroughs in the development of photocatalytic materials are strongly desired.

While our industries are constantly providing a variety of new products and materials based on innovative new technologies, it is also becoming imperative to develop better methods of recycling and treating waste materials as well. Moreover, we need to reduce consumption of our limited natural resources and raise awareness of the great impact such consumerism has on our environment. To address such issues, organic polymer semiconducting materials such as graphitic-like polymer carbon nitride (generally named as g-C_3N_4 for simplicity) and hexagonal boron carbon nitride (h-BCN) have been investigated as new families of promising visible light–responsive photocatalytic materials.

In this book, current developments in photocatalysis from inorganic semiconducting photocatalytic materials such as TiO_2, $SrTiO_3$, and $BiVO_4$ to organic semiconducting polymer materials such as g-C_3N_4 and h-BCN materials are summarized. Special attention has been focused on a clarification of the reaction mechanisms at the molecular level, the construction and optimization of these photocatalytic materials, and their

application to solar energy conversion systems such as the decomposition of H_2O, fixation of CO_2, and degradation of various toxic compounds in the air and water. Such developments in safe and clean energy production technologies can be considered one of the most exciting and important research trends for the 21st century and beyond.

Editors
Xinchen Wang
Masakazu Anpo
Xianzhi Fu

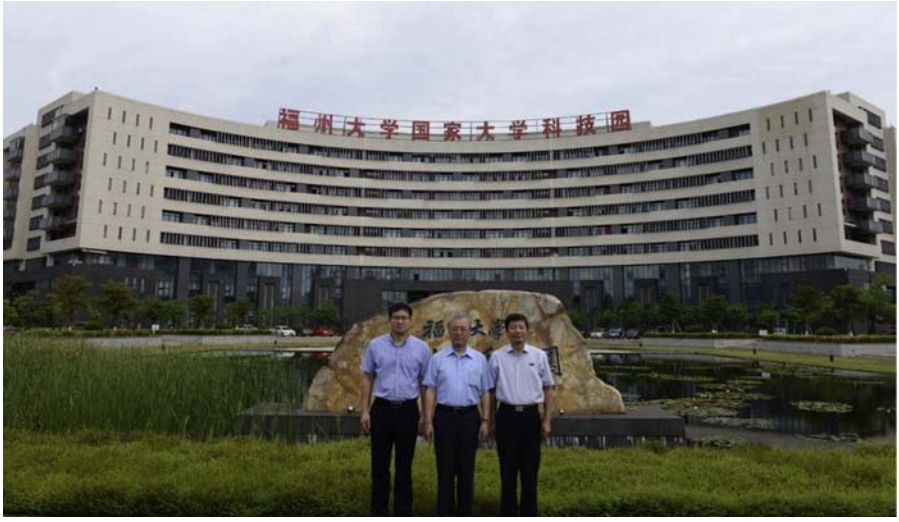

(Xinchen Wang (left), Masakazu Anpo (middle), and Xianzhi Fu (right) at the front of the Research Institute of Photocatalysis, Fuzhou University, July 5, 2019)

Seizing solar hydrogen from water promoted by magic spin transporting, chiral-induced spin state−selective filtering, and upconversion

13

Wenyan Zhang [1], *Gongxuan Lu* [2]
[1]College of Material Engineering, Jinling Institute of Technology, Nanjing, China; [2]State Key Laboratory for Oxo Synthesis and Selective Oxidation, Lanzhou Institute of Chemical Physics, Chinese Academy of Sciences, Lanzhou, China

1. Introduction

Hydrogen is a green energy with high enthalpy and zero environmental pollution. Photocatalytic hydrogen evolution (HER) is a sustainable and promising way to generate hydrogen [1−5]. Despite great achievements in photocatalytic HER research, its efficiency is still limited due to undesirable electron transporting efficiency, high overpotential, and low stability of some photocatalysts so that they have poor performance in resisting photocorrosion and poisoning of by-product [2−6]. In recent years, many investigations have shown strong evidences for spintronic effects on enhancing photocatalytic HER.

Firstly, theoretical and experimental investigations both validate that dissipationless spin transporting is an effective route to promote electron transfer efficiency in suitable spin transfer medium [7]. In some cases, spin transfer medium could even exhibit superconducting performance due to dissipationless spin-polarized currents [3]. 2D transfer media like graphene and some semiconductors like $SrTiO_3$ and $La_{1-x}Sr_xMO_3$ are all promising candidates for spin transportation. As a result, it is possible to realize photoelectron spin polarizing and transporting in photocatalytic HER system, for 2D transfer media and semiconductor are both significant components of photocatalysts. Some researchers applied heavy atom effect and magnetic induction effect to induce photoelectron spin polarizing in photocatalytic system. Spin transfer in catalyst resulted in larger photocurrents (at least two times) and better HER turn-over frequency (up to 200%) in photocatalytic system [2−8].

The second strategy is by chiral-induced spin selectivity (CISS) effect. Studies show that controlling spin state of OH• radicals in photocatalytic cell can not only decrease OER overpotential (even to 0 eV) of water splitting but also improve stability and lifetime of photocatalysts. Several strategies have been developed for aligning spin state of

Current Developments in Photocatalysis and Photocatalytic Materials
https://doi.org/10.1016/B978-0-12-819000-5.00013-8

OH• by utilizing chiral molecules to spin filter photoelectrons; therefore, electron polarization can approach 74%, which is significantly larger than some traditional transition metal devices. Besides, based on those achievements, we discuss challenges and developing trends of spintronic-enhanced photocatalytic HER research, expecting to provide valuable information to comprehend and explore such an interdisciplinary field.

Thirdly, upconversion (UC) material has attracted much attention because of its fantastic energy transfer capability of converting the low-energy photons into high-energy photons via anti-Stokes process. Among UC materials, the visible-to-UV UC materials exhibit remarkable potential in laser conversion, photocatalysis, the photocatalytic sterilization, and photocatalytic antibiosis in hygiene areas because of their capability of converting the visible radiation into ultraviolet emission. Moreover, UC process can provide a new route to upconvert infrared light to visible light, which can be used by visible light-sensitive semiconductor to generate hydrogen. This route presents a possible way to use about 50% infrared light to generate hydrogen instead of heating. This work focus on the current state of visible-to-UV UC materials and challenges in theoretical and commercial perspective.

2. Inducing spin transfer in photocatalytic system to promote hydrogen evolution

2.1 *Heavy atom–induced charge intersystem crossing relaxation*

In a typical sensitized HER photocatalyst composed of semiconductors, dye sensitizer, two-dimensional (2D) transfer media (such as RGO and g-C_3N_4), and cocatalysts [9], singlet and triplet state photoelectrons are generated from excited EY dye molecules by visible light irradiation, then migrate into RGO due to effective energy matching between excited dye and RGO, and reduce protons to hydrogen when they encounter cocatalysts on RGO (see Fig. 13.1). Given that singlet state photoelectrons spin antiparallel while triplet state photoelectrons spin parallel, spin polarizing those photoelectrons

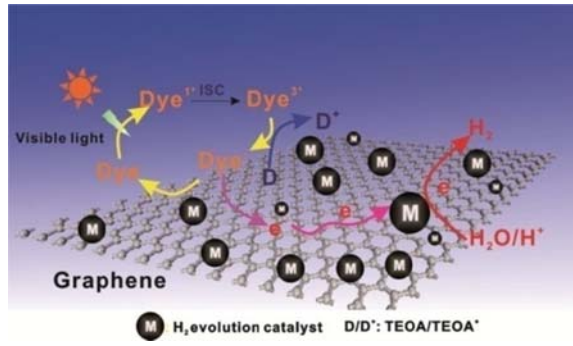

Figure 13.1 Proposed photocatalytic mechanism for efficient H_2 evolution over a xanthene dye–sensitized graphene/metal photocatalyst under visible light irradiation [9].

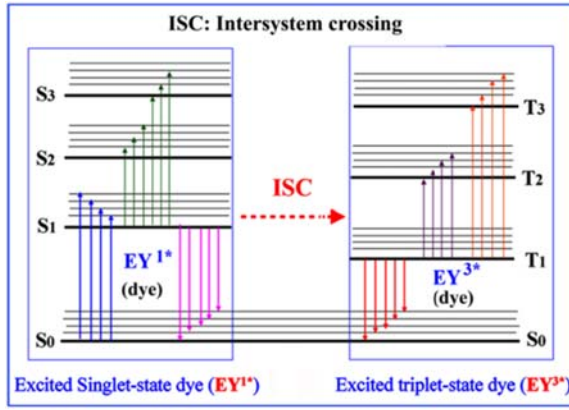

Figure 13.2 Modified Jablonski diagram for electron intersystem crossing (ISC) relaxation from excited singlet state to excited triplet state [10].

could be realized if one can enlarge intersystem crossing (ISC) relaxation probability to promote singlet state electrons relaxing to their triplet state (illustrated in Fig. 13.2). However, ***ISC*** relaxation probability is very low due to spin-forbidden rules, so some strategy should be done to break the spin-forbidden rule [2,10].

Heavy atom can break spin-forbidden rules on ***ISC*** relaxation of dye (called heavy atom effect) and result in spintronic-enhanced photocatalytic HER [2,3,8]. Lu et al. found that heavy atom−induced large spin−orbit (***SOC***) interaction is effective for breaking spin-forbidden ***ISC*** relaxation [2]. As illustrated in Fig. 13.3, they decorated

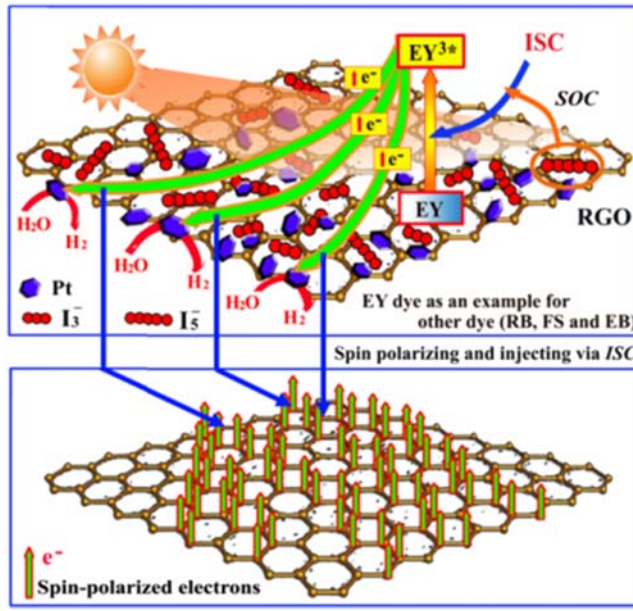

Figure 13.3 Iodine atom−induced spin polarizing and injecting in photocatalytic HER reaction [2].

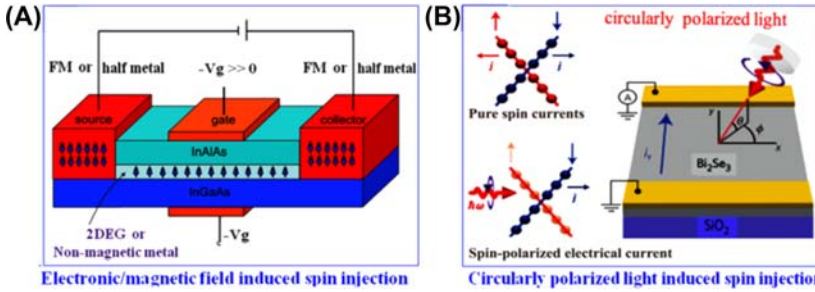

Figure 13.4 Two methods for spin polarizing and injecting induced, respectively, by (A) external electronic/magnetic field and (B) circularly polarized light [12].

iodine heavy atoms on RGO sheets as a transfer media to facilitate electron spin polarizing and injection into RGO sensitized, respectively, by Rose Bengal (RB), Fluorescein sodium (FS), and Erythrosin B (EB) dye. Because of their high nuclear charges, heavy atoms can induce ***SOC*** interaction between the electrons' spin and their orbital motion around the nucleus to break the spin-forbidden rules for ***ISC*** relaxation. Optical and electronic tests provide additional evidences of photoelectrons polarizing to form spin-polarized currents, for iodine atoms promoted ***ISC*** relaxation via strong ***SOC*** interaction. The turn-over frequency (TOF) of HER was enlarged up to 200% with better photoelectron transfer efficiency.

Heavy atom-***induced*** ISC relaxation is especially convenient and suitable for spin transfer in liquid photocatalytic reaction system, compared with tranditional methods which commonly induce spin polarizing by strong electronic/magnetic field (Fig. 13.4A) or circularly polarized light (Fig. 13.4B) [11,12], as both methods require special instruments so their complexity and cost are increased. In contrast, heavy atom−induced ***ISC*** relaxation does not need any instruments.

2.2 Heavy atom−induced electron spin-flip and tunneling

Heavy atoms are also capable of generating strong Rashba spin-orbit coupling (***SOC***) on 2D transfer media to make the transferred electrons flip to spin parallel, thus promoting the spin polarizing degree of photocurrents [2,3,8]. Partially fulfilled p or d orbits of heavy atom could form hybrid orbits with 2D transfer media, and that transferred electrons can tunnel on the 2D transfer media by hopping through those hybrid orbits [7].

As illustrated in Fig. 13.5A, RGO honeycomb lattice is constructed by carbon atoms which form σ and π bonds by sp^2 hybridization of 2s orbits and 2p orbits [7]. The semimetal property of RGO is mainly ascribed to the contribution of 2p orbits. When heavy atom clusters are assembled on RGO (Fig. 13.5B), their high nuclear charges induce Rashba ***SOC*** on RGO. Because of the reflection symmetry to the lattice plane, only the ***SOC*** in the normal direction ($L_z\sigma_z$) has nonzero contribution to electron flipping [3,7]. Therefore, the Hamiltonian of heavy atom−decorated RGO could be simplified and described as Formula 13.1:

$$H = H_{SO}^{R} + \delta H \tag{13.1}$$

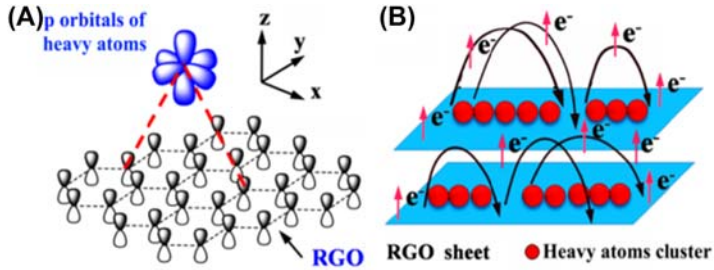

Figure 13.5 Scheme of (A) electrons' tunneling with the aids of heavy atom p orbitals and (B) electron spin-flip and tunneling on RGO due to Rashba ***SOC*** induced by heavy atom [2].

where H^{R}_{SO} corresponds to Rashba ***SOC*** on RGO, and δH corresponds to the dependence of electron hopping energy on impurity, defects, and sp^3 distortion in RGO lattices.

Rashba ***SOC*** on RGO induce a coupling between first neighbors with opposite spin, which could be described as Formula 13.2

$$H^{R}_{so} = i\lambda \sum_{<i_A j_B>,\sigma,\sigma'} \left(\hat{\mu}_{i_A j_B}\right)_z |Z,i_{A,}\sigma> <Z,j_{B,}\sigma'| \tag{13.2}$$

$\hat{\mu}_{i_A j_B}$ is the unit parallel vector, σ is the electron spin Pauli matrices, and $|Z,i_{A,}\sigma>$ represents the wave function of an electron which occupies a carbon p_z orbits.

δH, the dependence of electron shopping energy, includes a spin-orbit coupling part and a crystal field H_{CF} term. Its Hamiltonian could be described by Formula 13.3:

$$\delta H = \Delta_{so} \overrightarrow{L} \bullet \rightarrow \sigma + H_{CF} \tag{13.3}$$

where Δ_{so} is the spin-orbit coupling parameter, $\overrightarrow{L}$ and $\rightarrow\sigma$ are the usual angular momentum and spin operators. Parameter $\overrightarrow{L} \bullet \rightarrow \sigma$ and H_{CF} could be described by Formula 13.4 and 13.5, respectively:

$$\overrightarrow{L} \bullet \rightarrow \sigma = 1/2 \begin{bmatrix} 0 & -i & 0 & 0 & 0 & 1 \\ -i & 0 & 0 & 0 & 0 & -i \\ 0 & 0 & 0 & -1 & i & 0 \\ 0 & 0 & -1 & 0 & i & 0 \\ 0 & 0 & -i & -i & 0 & 0 \\ 1 & i & 0 & 0 & i & 0 \end{bmatrix} \tag{13.4}$$

$$\left(\left\{|p_x\uparrow>, |p_x\downarrow>, |p_y\uparrow>, |p_y\downarrow>, |p_z\uparrow>, |p_z\downarrow>\right\}\right)$$

$$H_{CF} = \begin{bmatrix} \varepsilon_x & 0 & 0 & 0 & 0 & 0 \\ 0 & \varepsilon_y & 0 & 0 & 0 & 0 \\ 0 & 0 & \varepsilon_z & 0 & 0 & 0 \\ 0 & 0 & 0 & \varepsilon_x & 0 & 0 \\ 0 & 0 & 0 & 0 & \varepsilon_y & 0 \\ 0 & 0 & 0 & 0 & 0 & \varepsilon_z \end{bmatrix} (\varepsilon_x = \varepsilon_y \neq \varepsilon_z) \tag{13.5}$$

Because of their high nuclear charge density, heave atoms on RGO induce irregular electric fields at their periphery. The irregular electric fields $\overrightarrow{E}$ could be described as Formula 13.6:

$$\overrightarrow{E} = \frac{1}{4\pi\varepsilon_0} \frac{Q}{r^2} \hat{r} \tag{13.6}$$

$\varepsilon_0 = 8.85 \times 10^{-12}\ \mathrm{C^2/(N^{-1} \cdot m^2)}$ is the vacuum dielectric constant, r is the distance between two charges, and $\mathrm{Q} = 1.602 \times 10^{-19}\mathrm{C}$ represents the point charge that is elementary charge.

The irregular electric field $\overrightarrow{E}$ could induce a large Rashba spin-orbit coupling to facilitate electron spin-flip and an idiosyncratic Hall conductivity. The Hall conductivity could be written as Formula 13.7:

$$\omega = \omega\uparrow + \omega\downarrow = 2\frac{e^2}{h} \tag{13.7}$$

where $\boldsymbol{\omega}$ is the Hall conductivity of material, $\omega\uparrow$ and $\omega\downarrow$ represent different directions of the spin, and $h = 6.626 \times 10^{-34}\mathrm{J \cdot s}$ is the Planck constant.

By assembling RGO with Au atoms, Marchenko et al. realize electron spin polarizing of those Au atom−induced giant spin-orbit splitting (up to 100 meV) to facilitate electron flip-flop [13]. Brey [7] and Miranda et al. [14], respectively, assembled Pb layer periodically on RGO (Fig. 13.6A) and discovered that Pb atoms can also trigger

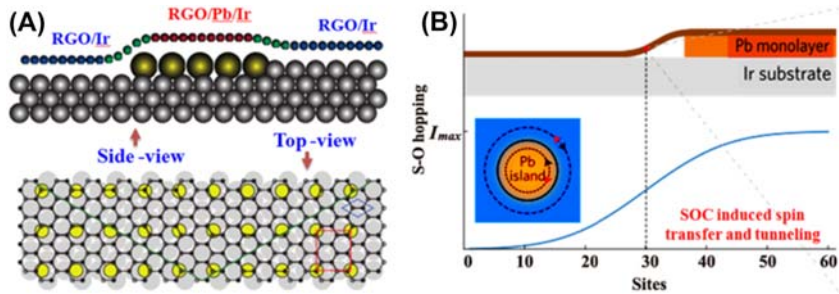

Figure 13.6 (A) Scheme of the atomic arrangement for RGO decorated by Pb atoms and (B) spatial evolution of the S−O coupling across the border of the Pb-intercalated regions [14].

quantum spin Hall effect for electrons by inducing giant Rashba-like ***SOC***, thus providing Pb-RGO composite layers with special electron transport nature (Fig. 13.6B). Lu et al. proved that Rashba ***SOC*** could be induced by iodine atoms not only on RGO but also on g-C_3N_4 sheets [8]. Iodide atom−decorated RGO and g-C_3N_4 exhibited better charge transfer performance due to spin transfer, tunneling, and higher HER rate and TOFs.

2.3 Electron transporting enhancement by magnetic-induced spin polarizing

Magnetic induction is capable of generating high Zeeman splitting energy to *polarize electrons spin states, thus regulating transporting performance of photoelectrons in transfer media* [2]. When magnetic field is enlarged from 1.75 to 27.5 T, the conductance of bilayer RGO increases from 10^{-1} e^2/h to 10^1 e^2/h with its transfer from antiferromagnetic phase to ferromagnetic phase (Fig. 13.7A) [15], due to magnetic-induced electron spin polarization on bilayer RGO (illustrated in Fig. 13.7B1 and B3). Antiferromagnetic phase has poor electron transfer capability as its LUMO and HOMO levels are split (Fig. 13.7B2). In ferromagnetic bilayer RGO, electron spin polarizing leads to counterpropagating of edge states, thus the LUMO and HOMO levels are intersected to result in better conductivity, even metallic conductance (Fig. 13.7B4), which can promote photocatalytic HER rate by enhancing electron transporting capability of RGO.

2.4 Important advantages of spin transportation in photocatalytic HER system

SOC intensity depends highly on the concentration of heavy atoms and their distributions in photocatalysts [2,3,8], thus one can enhance spin transfer efficiency conveniently by

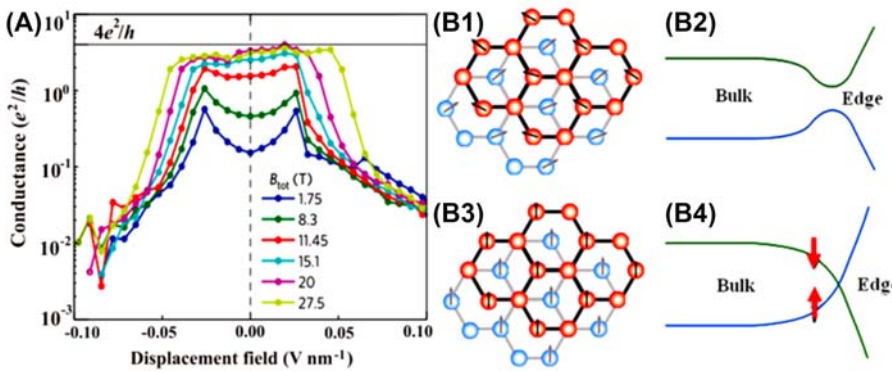

Figure 13.7 Magnetic-induced spin transfer on bilayer RGO and the topological structure of bilayer. (A) Spin conductance variation with magnetic field; illustrations of spin and pseudo spin configurations for antiferromagnetic phases (B1) and ferromagnetic phases (C1), in the BLG $\nu = 0$ state; Diagram of predicted bulk and edge energy levels for antiferromagnetic phases (B2) and ferromagnetic phases (C2) [15]; (red balls: carbon atoms on one RGO layer; blue balls: carbon atoms on the other RGO layer).

regulating the type and distribution of heavy atoms on photocatalysts. Based on Raman, XPS characterization, and theoretical calculation, Lu et al. found that the I atoms exist as I_3^- and I_5^- clusters on the RGO sheets (see Fig. 13.8). I_3^- has two different geometries, the linear chain and triangle chain, while the ground-state energy of linear chain is about 0.001 eV lower than that of triangle species. The I_5^- also has two different geometries, the linear chain and planar square. Similarly, linear chain of I_5^- is more stable as it has lower ground-state energy than planar square geometry. Therefore, the I_3^- and I_5^- clusters exist as linear chain structure which were randomly placed on RGO sheets. HER reached the maximum when I/Cmol% was 1. As for I atom-decorated g-C_3N_4, results showed that I atoms also exist as I_3^- and I_5^- linear chain clusters on g-C_3N_4 sheets, located in C1−C2 and C4−C5 directions (Fig. 13.9). Electrons in C1 or C4 could tunnel through the p orbitals of I_3^- and I_5^- clusters to C2 and C5, thus promoting electron transferring and separating capability of g-C_3N_4 sheets and promoting HER [8]. Photocurrents were enlarged at least two times because of spin polarizing of photoelectrons.

Placing Pb atoms in hollow positions of carbon atoms in RGO could open energy gap at its Dirac points, inducing spin-conserving intrinsic like ***SOC*** for RGO (Fig. 13.10A1 and A2 [7]). In that case, energy gap increased linearly proportional to the density of Pb atoms and could reach 100 meV when Pb atom concentration rose up to 20% of the carbon atom. Placing Pb atoms on top of carbon atoms not only induced spin-conserving intrinsic like ***SOC*** but also resulted in Rashba-like spin-flip hopping for RGO (Fig. 13.10B1 and B2). d orbits of Pb atoms were hybridized with carbon atoms to form hybridized orbit, so electron migration was effectively promoted because they could hop and tunnel through RGO.

As for Au atom-decorated RGO, their spin-orbit splitting was only 9 meV near E_F (Fermi energy) when the Au atom layer was far from RGO (Fig. 13.11A) [13]. In this case, the A-B symmetry of carbon atoms were broken in the on-top geometry if they put Au atoms on top of carbon atoms and that induced large ***SOC*** interaction to open energy gap (up to 40 meV) at its Dirac points. The A-B symmetry of carbon atoms could be preserved if they place Au atoms in hollow sites of carbon atoms (Fig. 13.11B). In that case, a giant ***SOC*** interaction (up to 70 meV) was generated and orbit hybridization was formed between 5d orbit of gold atoms and p orbit of carbon atoms. Hollow sites of carbon atoms are suitable place for Au atoms to generate large ***SOC*** with 60 meV even when Au atom ratio was reduced to 25% (Fig. 13.11C).

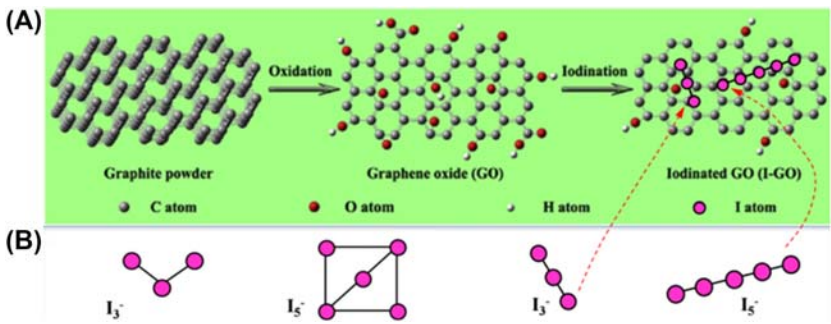

Figure 13.8 (A) Schematic diagram of preparing of I atoms decorated RGO; (B) Scheme of I_3^- and I_5^- cluster isomers with different energy calculated by density functional theory (DFT) [3].

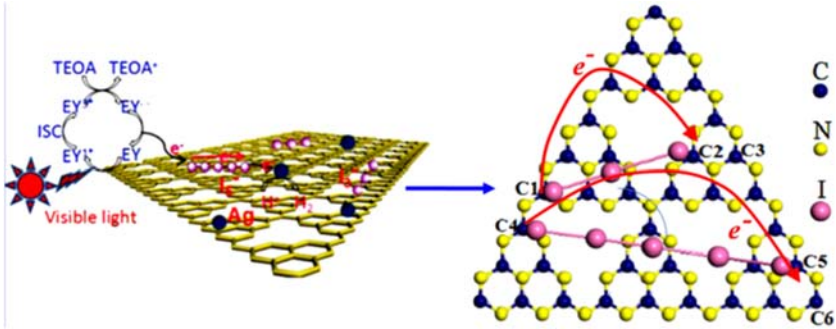

Figure 13.9 Spin transfer and tunneling on g-C_3N_4 via the aids of p orbital of polyiodides [8].

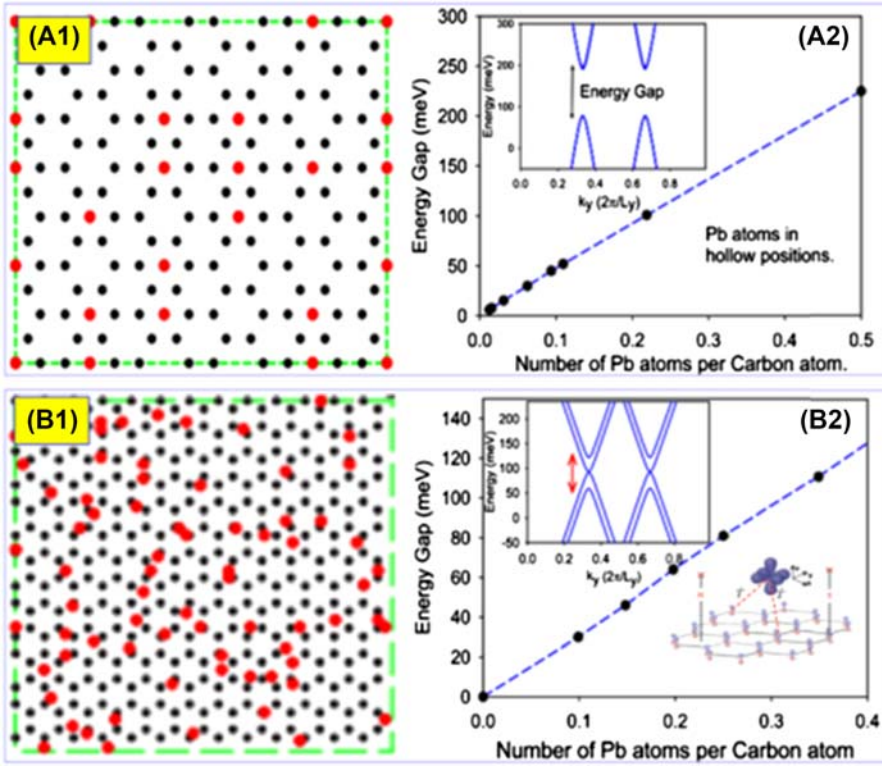

Figure 13.10 (A1) Pb atoms in hollow positions of RGO; (A2) energy gap and Dirac points of RGO [7]; (B1) Pb atoms on Top of RGO; (B2) energy gap and Dirac points of RGO [12].

2.5 Challenges of applying spin transfer strategy in photocatalytic HER system

The challenges are still remained, such as to uncover mechanism of spin transfer in complex environment, lack of appropriate characterization, especially real-time detection, and design low-cost techniques to synthesize nano-scaled photocatalysts for

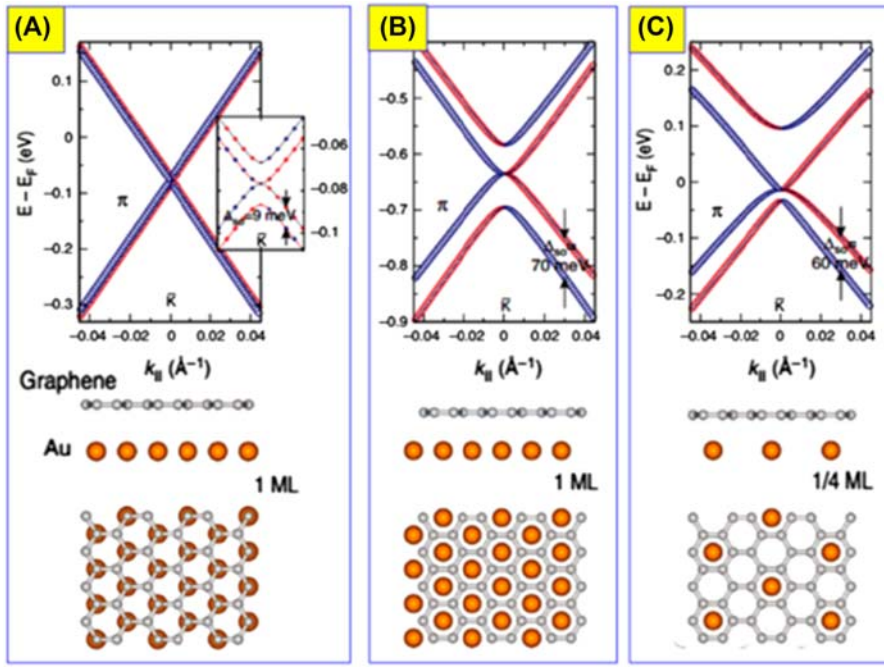

Figure 13.11 Effect of Au atom concentration and distribution on spin transfer and electron tunneling for Au-decorated RGO sheets: (A) Au (orange circle [gray in print version]) atoms on top of carbon atoms, (B) Au atoms in hollow sites of carbon atoms, (C) reducing Au atom numbers in hollow sites of carbon atoms [13].

spintronic-enhanced photocatalytic HER. Besides, present spintronic theories may not be suitable for photocatalytic HER due to the complication of liquid photoatalytic enviroment, so new model based on real reaction environment is highly demanded. Furthermore, there is a lack of real-time spin detection and sensing techniques with high testing accuracy. Additionally, it is still hard to prepare nano-scaled photocatalysts for spintronic-enhanced photocatalytic HER, for molecular beam epitaxy and nanoimprint lithography are complex and high cost.

3. Chiral-induced spin selectivity effect on promoting water-splitting effect

3.1 Chiral-induced spin selectivity theory and its application in water splitting

Chiral molecules have a special capability of "filtering" the spin state of electrons. As illustrated in Fig. 13.12A, electrons will be spin polarized when they pass through helical electric field of chiral molecules, and that effect is called CISS effect [16,17]. CISS-induced electron polarizing in decorated with proteins, DNA molecules, and helicenes [18,19]. By chiral-induced spin filtering, electron polarization can approach 74%, which is significantly larger than some traditional transition metal devices.

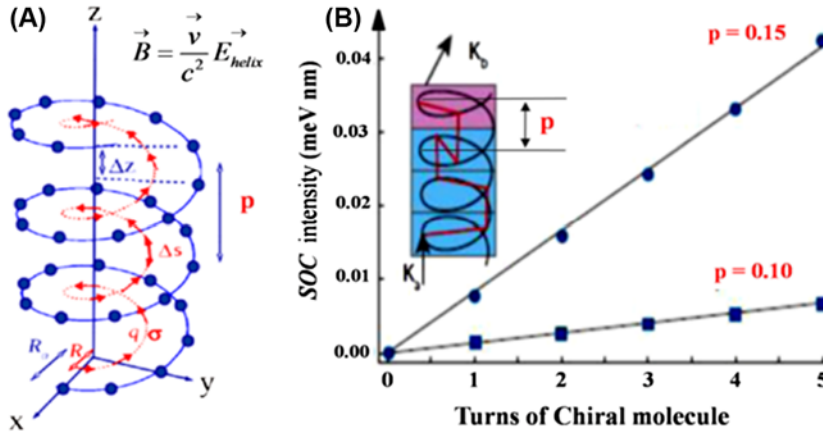

Figure 13.12 (A) An electron migrating through the helical electric field of a chiral molecule (B) dependence of spin-orbit coupling (SOC) intensity on helical electron field of chiral molecules [18].

As shown in Fig. 13.12A, supposing an electron passing through the helical electric field ($\overrightarrow{Ehelix}$) of a chiral molecule, $\overrightarrow{Ehelix}$ will induce a magnetic field ($\vec{B}$) in rest frame of the electron, and $\vec{B}$ could be described as Formula 13.9 [18]:

$$\vec{B} = \frac{\vec{v}}{c^2} \overrightarrow{Ehelix} \tag{13.9}$$

In Formula 13.9, $\vec{v}$ is the electron's velocity, and c is the speed of light.

Based on Formula 13.9, *the magnetic field ($\vec{B}$) can generate enough large spin-orbit coupling (SOC) interaction between the electron and atom nuclei of the chiral molecule* [18]. For instance, supposing an electron moves in a 4.5×10^{11} V m^{-1} helical electric field ($\overrightarrow{Ehelix}$), 3T magnetic field can be generated even when $\vec{v}$ is only 0.2% of the speed of light. Therefore, hamiltonian of ***SOC*** interaction could be described as Formula 13.10, which originates directly from Pauli equation.

$$H_{SO} = \lambda \vec{\sigma} \left(\vec{p} \times \overrightarrow{Ehelix} \right) = \lambda \vec{\sigma} \left(\vec{p} \times \frac{\vec{B} c^2}{\vec{v}} \right) \tag{13.10}$$

$$\lambda = (e\hbar) / \left(4m^2 c^2\right)$$

where $\vec{p}$ is the electron's migrating momentum, $\vec{v}$ is the electron's velocity, and m is electron mass, c is the speed of light. $\vec{\sigma}$, which expresses electron spin state, is a vector whose components are the Pauli matrices of σx, σy, and σz.

When electrons move in magnetic field $\vec{B}$, they will be spin polarized by large SOC generated between the electrons and chiral molecules. From Formula 13.10, it is also obvious that the ***SOC*** interaction depends highly on the intensity and direction of helical electric field $\overrightarrow{Ehelix}$. Meanwhile, $\overrightarrow{Ehelix}$ is closely related to the structure of chiral molecule, relying on their turns and magnitude along p_z, as shown in Fig. 13.12B.

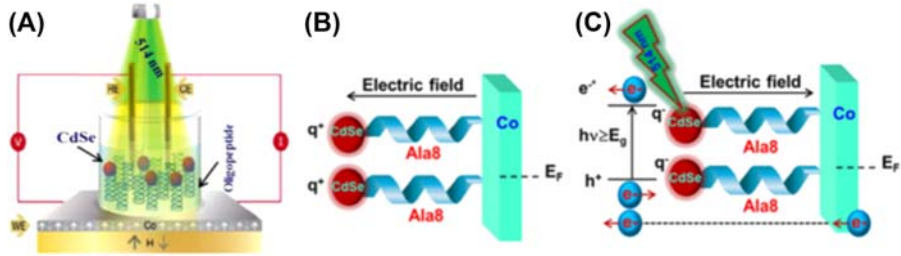

Figure 13.13 (A) Schematic illustrating the setup used for the light-controlled spin-dependent electrochemical measurements across AL8-CdSe NPs assemblies. Working electrode was magnetized "UP" or "DOWN" (white and yellow arrows [light gray in print version], respectively) during the electrochemical measurements. The CdSe NPs were excited by a green laser ($\lambda exc = 514$ nm). (B) Before photoexcitation, the CdSe-NPs are positively charged and electrons are transferred with their spin aligned parallel to their velocity. (C) During photoexcitation, the NPs become negatively charged. The electric field on the AL8-CdSe is in the opposite direction and thus the electrons with spin antiparallel to their velocity are preferentially transferred [20].

Therefore, it is potential to enhance ***CISS*** efficiency by choosing suitable chiral molecules to improve electron spin polarizing degree.

3.1.1 CISS *effect of spin polarizing on photocatalytic HER*

Assembled a series of chiral molecules onto different photocatalysts like CdSe (Fig. 13.13A[20]), TiO_2 [24] and metallic materials like Ag (Fig. 13.14A), Au (Fig. 13.14B), and Ni layer (Fig. 13.13B and C) provided that photoinduced electrons or holes were spin polarized due to ***CISS*** effect on spin filtering [21]. Spin polarizing degree of photoelectrons depends on chiral molecule structure.

3.2 *Essential advantages of* CISS *effect on promoting water splitting*

3.2.1 CISS *can lower down water-splitting overpotential for HER and prolong the photocatalysts lifetime by* CISS *effect*

Splitting water for HER often encounters high overpotential due to large overpotential needed for water oxidation (OER). *Current researches have revealed strong evidences that side reactions of H_2O_2 yielding is a significant reason for high overpotential of water-splitting reaction* [22−23]. Water-splitting overpotential roots from restrictions on the electrons' spin in generating a ground-state triplet oxygen molecule. It is suggested that two spin-paralleled hydroxyl radical intermediates (OH•) combine to form triplet state O_2 (Fig. 13.15A and B) in photocatalytic water splitting, while two spin antiparallel OH• radicals are prone to form singlet-state H_2O_2, so a promising way to decrease overpotential and inhibit side reactions of H_2O_2 yield is to polarize OH• spin state during water-splitting reactions by coating anode with chiral molecules, which can spin filter photo-electrons via ***CISS*** effect, as Ron et al. proposed [22−24].

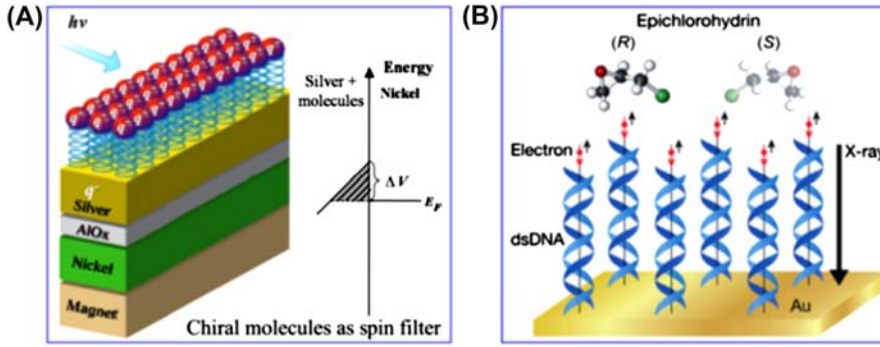

Figure 13.14 (A) Scheme and energy state diagrams of photocatalyst/device designed for realizing CISS-induced spin filtering for photogenerated electron. The photocatalyst/device designed by assembling chiral molecules on Ag/AlOx/Ni multilayers; (B) diagram showing how the secondary electrons produced by X-ray irradiation become spin-polarized, with their spins aligned antiparallel to their velocity, and induce chiral selective chemistry in adsorbed (R)- or (S)-epichlorohydrin.

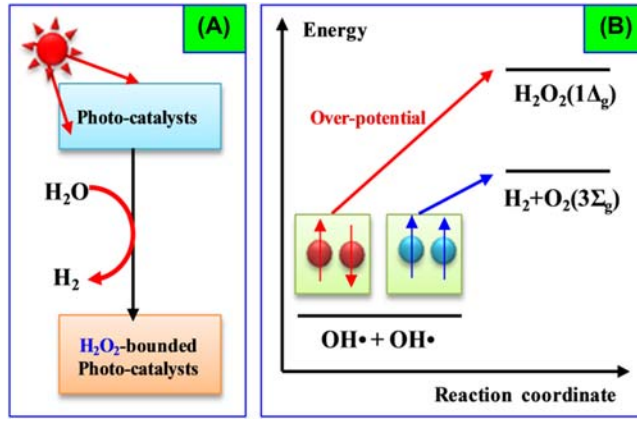

Figure 13.15 (A) Illustration of photocatalytic reaction to generate O_2 and H_2O_2 by-products and (B) energy level illustration of overpotential on producing O_2 and H_2O_2 by-products [22–24].

Controlling spin state of OH• radicals can lower down OER overpotential by inhibiting side reaction of H_2O_2 yield [3]. Ron and Mtangi et al. fulfilled it by ***CISS***-induced electron spin filtering in water-splitting reaction system [22–24]. As illustrated in Fig. 13.16A and B, they assembled CdSe and TiO_2 photocatalysts with chiral molecules which have helical electric field to spin filter photogenerated photoelectrons via ***CISS*** effect to prove the effect of spin aligning on reducing OER potential and enhancing HER efficiency. OER overpotential decreased obviously on photocatalysts decorated with chiral molecules, decreased 0.17 eV with AL5 and AL7, and *even was reduced to 0 V* when coating photocatalysts with DNA molecules (Fig. 13.17A). In contrast, OER overpotential was higher than 0.5 eV decorated with achiral molecules of 4-MBA, MPA, and MUA (Fig. 13.17B).

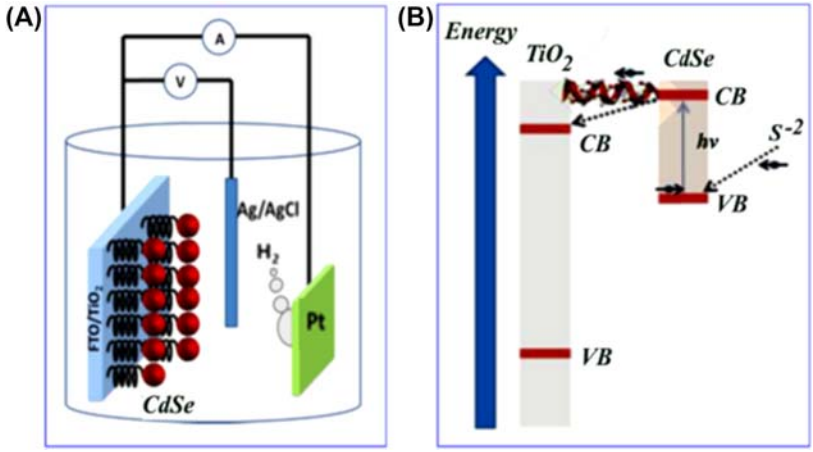

Figure 13.16 (A) Photoelectrochemical cell designed for realizing ***CISS***-induced spin filter in photocatalytic water splitting. The cell composed by CdSe nanoparticles, TiO_2 nanoparticles, chiral molecules, and FTO and Pt electrode. (B) Energy level scheme for the designed cell [23].

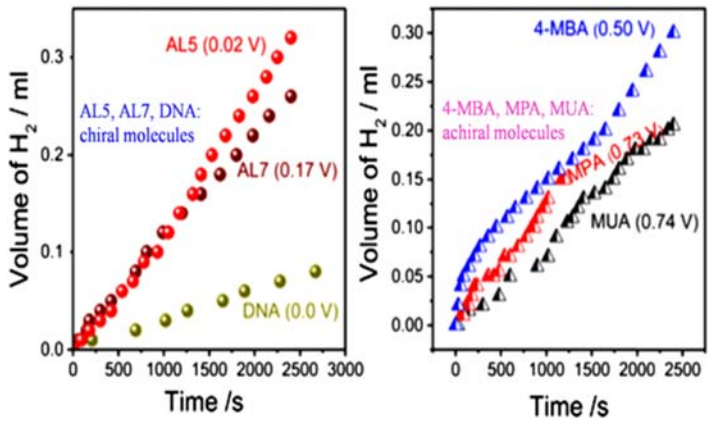

Figure 13.17 Time-resolved hydrogen evolution over photocatalysts coated with (A) chiral molecules and (B) achiral molecules [23].

Moreover, in their investigation, H_2O_2 detection proved that spin aligning of OH• radicals via CISS effect can effectively inhibit the H_2O_2 production as well. That is good for improve the stability and lifetime of photo/electronic catalyst, considering that H_2O_2 detection proved that spin aligning of OH• radicals via CISS effect also resluted in lower H_2O_2 production [22−24]. As shown in Fig. 13.18A and B, H_2O_2 were produced over bare TiO_2 and TiO_2 coated by achiral molecule A-Zn and A-TPyA, while little H_2O_2 were generated on TiO_2 decorated by chiral molecule S−Zn and

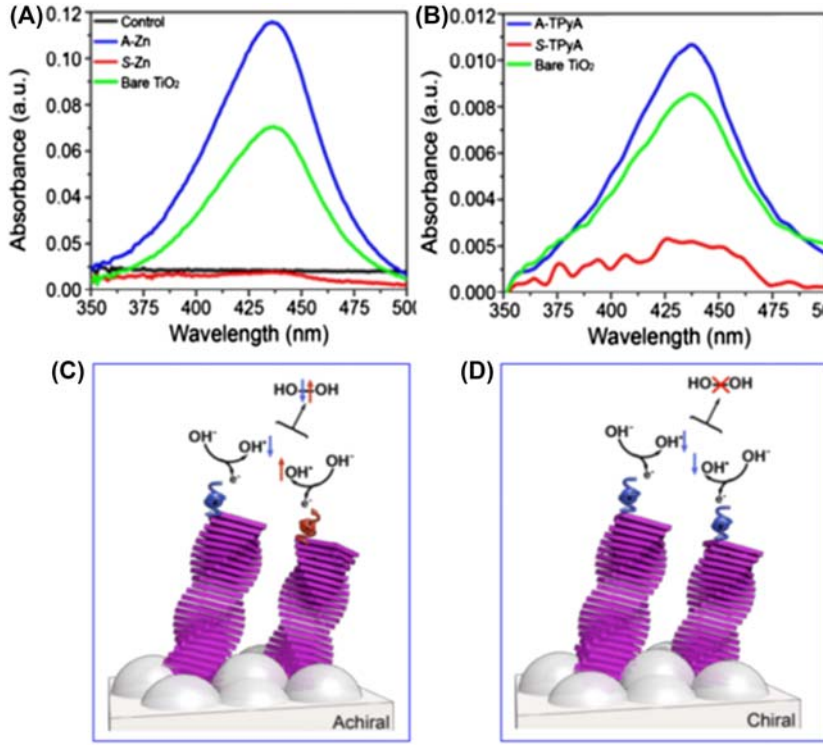

Figure 13.18 UV-vis absorption spectra from the titration of electrolyte (Na_2SO_4) with o-tolidine of bare TiO_2 and TiO_2 electrodes coated with (A) self-assembled Zn-porphyrins of achiral (A-Zn) and chiral (S−Zn); (B) TPyA molecules of achiral (A-TPyA) and chiral (S-TPyA). The control refers to the titration of unused Na_2SO_4 with o-tolidine; (C) two spin antiparalleled electrons on anode facilitating the yield of two spin antiparallel OH•, which interact to form singlet H_2O_2; (D) Two spin-paralleled electrons on anode facilitating the yield of two spin aligned OH•, which interact to form triplet O_2 [24].

S-TPyA. The mechanism is shown Fig. 13.18C and D. For TiO_2 coated by achiral molecule (Fig. 13.18C), photogenerated OH• radicals were not spin polarized and two antiparallel OH• interacted to produce H_2O_2. For TiO_2 coated by chiral molecule (Fig. 13.19D), photogenerated OH• radicals were spin polarized and they interacted to yield triplet O_2.

4. The important role of upconversion material in promoting water oxidation

In recent years, UC material has attracted much attention because of its fantastic energy transfer capability of converting the low-energy photons into high-energy photons via anti-Stokes process [25,26]. Two or more photons were absorbed sequentially by a material to reach an excited state, which could release one higher-energy photon then, such

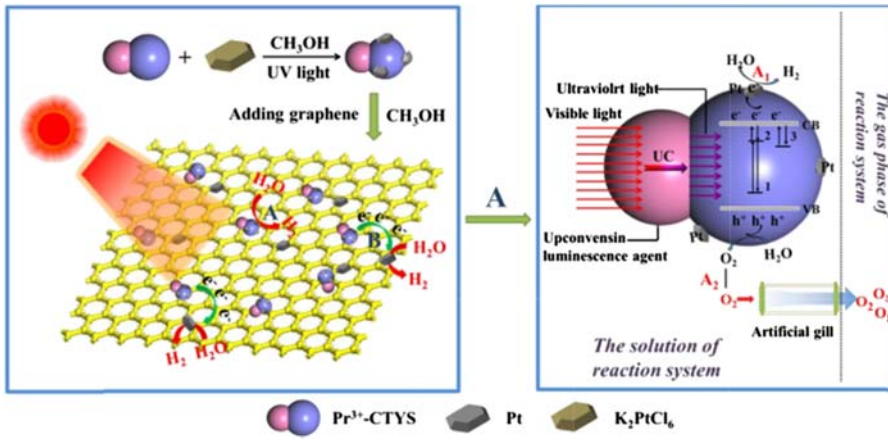

Figure 13.19 Photocatalytic mechanism of hydrogen evolution over $CaTiO_3/Pr^{3+}—Y_2SiO_5$/RGO catalyst [29].

as IR-to-visible light, visible-to-UV light and visible-to-higher energy visible. UC converting efficiency depends highly on the dopping tolerance, refractive index, phonon energy and chemical stability of matrix [27]. Given current stable TiO_2 and Ti-based photocatalysts mainly respond to UV irradiation, and sulfide and Selenide-based photocatalysts could work under visible light irradiation, one can combing the advantages of these UV-responsive and visible-light-responsive photocatalysts by applying visible-to-UV UC material as bridge to promote visible light—driven water splitting.

Recently, Lu et al. successfully explored aforementioned strategy by combining Pr^{3+}-CTO with the visible-to-ultraviolet UC unit for water splitting. The visible-to-ultraviolet UC unit was able to transfer incident visible radiation to UV light emission. Owing to large area of heterojunction constructed between the visible-to-ultraviolet UC unit and UV-responsive photocatalyst, the yielded UV light was utilized successfully by the UV-responsive photocatalyst (Fig. 13.19) [28,29]. The photocatalytic activity for hydrogen generation has been raised up to 480% with excellent stability in three recycle reactions and charge lifetime was also prolonged.

Consequently, it could be expected that the visible-to-ultraviolet UC materials will play important theoretical and commercial role in photocatalytic research fields by assembling them with UV-responsive photocatalysts. The convenient strategy has good versatility for most UV-responsive photocatalysts to realize overall split water by visible light irradiation.

5. The future of spin transfer, CISS effect, and upconversion strategies on promoting water splitting

Until now, plenty of scientific evidences show positive effect of spintronics on enhancing photocatalytic HER. On one hand, triggering the spin polarizing

and transporting of photoelectron can result in more efficient photocurrent transfer for HER reactions. On the other hand, spin aligning of OH• is found to be effective to decrease OER overpotential and reduce by-product yield during water splitting reaction, and this maneuver has been realized by ***CCIS***-induced spin filtering and polarizing in photo/electronic catalytic systems. Despite these advantages, spintronic-enhanced photocatalytic HER still meets several obstacles including developing and innovating intrinsic mechanisms, constructing real-time sensing and monitoring detection device, as well as developing more efficient and economic synthesis techniques and instruments for spintronic photocatalysts. Fortunately, modern spintronic achievements in topological insulator, quantum spin Hall effect, and chiral interface growth shed new light on tackling those obstacles. Based on its intrinsic advantages and big achievements, it is reasonable to expect the interdiciplinary research of photo/electronic catalysis and spintronic science will have gorgeous furture. Meanwhile, owning to its ability to manipulate and convert light energy, the visible-to-UV UC or even infrared-to-visible light materials possess huge potential in solar light−driven water-splitting fields to facilitate higher efficiency for HER, OER, and overall splitting water (for example $> 15\%$) when combing them with high efficient UV-responsive photocatalysts. More than expectations, the strong interactions between electron, charged atom (i.e., hydride), and nuclei can lead to unexpected low-energy nuclear reaction or even nuclear transmutations under very mild conditions (for example, potassium to calcium transmutation) [30−33]. All those efforts make resolving the worldwide energy crisis and accompanied environmental problems promising.

Acknowledgments

This work is supported by the NSFC (51802130 and 21433007).

References

[1] A.J. Bard, M.A. Fox, Artificial photosynthesis-Solar splitting of water to hydrogen and oxygen, Acc. Chem. Res. 28 (1995) 141−145.
[2] W.Y. Zhang, G.X. Lu, The enhancement of electron transportation and photocatalytic activity for hydrogen generation by introducing spin-polarized current into dye-sensitized photocatalyst, Catal. Sci. Technol. 6 (2016) 7693−7697.
[3] X.Q. Zhang, G.X. Lu, The spin-orbit coupling induced spin flip and its role in the enhancement of the photocatalytic hydrogen evolution over iodinated graphene oxide, Carbon 108 (2016) 215−224.
[4] Z. Li, Q. Wang, C. Kong, et al., Interface charge transfer versus surface proton reduction: which is more pronounced on photoinduced hydrogen generation over sensitized Pt cocatalyst on RGO? J. Phys. Chem. C119 (2015) 13561−13568.

[5] C. Kong, S. Min, G. Lu, Dye-sensitized cobalt catalysts for high efficient visible light hydrogen evolution, Int. J. Hydrogen Energy 39 (2014) 4836−4844.
[6] C. Kong, S. Min, G. Lu, Dye-sensitized NiSx catalyst decorated on graphene for highly efficient reduction of water to hydrogen under visible light irradiation, ACS Catal. 4 (2014) 2763−2769.
[7] L. Brey, Spin-orbit coupling in graphene induced by adatoms with outer-shell p orbitals, Phys. Rev. B. 92 (2015) 235444.
[8] Z. Li, B. Tian, W. Zhang, et al., Enhancing photoactivity for hydrogen generation by electron tunneling via flip-flop hopping over iodinated graphitic carbon nitride, Appl. Catal. B Environ. 204 (2017) 33−42.
[9] S.X. Min, G.X. Lu, Dye-sensitized reduced graphene oxide photocatalysts for highly efficient visible-light-driven water reduction, J. Phys. Chem. C 115 (2011) 13938−13945.
[10] A. Kamkaew, S.H. Lim, H.B. Lee, et al., BODIPY dyes in photodynamic therapy, Chem. Soc. Rev. 42 (2013) 77−88.
[11] J. Zhao, W. Wu, J. Sun, et al., Triplet photosensitizers: from molecular design to applications, Chem. Soc. Rev. 42 (2013) 5323−5351.
[12] P. Chuang, S.C. Ho, L.W. Smith, et al., All-electric all-semiconductor spin field-effect transistors, Nat. Nanotechnol. 10 (2014) 35−39.
[13] D. Marchenko, Varykhalov, M.R. Scholz, et al., Giant Rashba splitting in graphene due to hybridization with gold, Nat. Commun. 3 (2012) 1232.
[14] F. Callejia, H. Ochoa, M. Garnica, et al., Spatial variation of a giant spin-orbit effect induces electron confinement in graphene on Pb islands, Nat. Phys. 11 (2015) 43−47.
[15] P. Maher, C.R. Dean, F. Young, et al., Evidence for a spin phase transition at charge neutrality in bilayer graphene, Nat. Phys. 9 (2013) 154−158.
[16] B. Gohler, V. Hamelbeck, T.Z. Markus, et al., Spin selectivity in electron transmission through self-assembled monolayers of double-stranded DNA, Science 331 (2011) 894.
[17] D. Mishra, T.Z. Markus, R. Naaman, et al., Spin-dependent electron transmission through bacteriorhodopsin embedded in purple membrane, Proc. Natl. Acad. Sci. USA 110 (2013) 14872.
[18] A.M. Guo, Q.F. Sun, Spin-dependent electron transport in protein-like single-helical molecules, Proc. Natl. Acad. Sci. U.S.A. 111 (2014) 11658.
[19] K.M. Alam, S. Pramanik, Spin filtering through single-wall carbon nanotubes functionalized with single-stranded DNA, Adv. Funct. Mater. 25 (2015) 3210−3218.
[20] P.C. Mondal, P. Roy, D. Kim, et al., Photospintronics: magnetic field-controlled photoemission and light-controlled spin transport in hybrid chiral oligopeptide-nanoparticle structures, Nano Lett. 16 (2016) 2806−2811.
[21] P.C. Mondal, N. Kantor-Uriel, S.P. Mathew, et al., Chiral conductive polymers as spin filters, Adv. Mater. 27 (2015) 1924−1927.
[22] W.Y. Zhang, K. Banerjee-Ghosh, F. Tassinari, R. Naaman, Enhanced electrochemical water splitting with chiral molecule-coated Fe3O4 nanoparticles, ACS Energy Lett. 3 (2018) 2308−2313.
[23] W. Mtangi, V. Kiran, C. Fontanesi, R. Naaman, Role of the electron spin polarization in water splitting, J. Phys. Chem. Lett. 6 (2015) 4916−4922.
[24] M. Wilbert, T. Francesco, V. Kiran, et al., Control of electrons' spin eliminates hydrogen peroxide formation during water splitting, J. Am. Chem. Soc. 139 (2017) 2794−2798.
[25] X.W. Liu, R.R. Deng, Y.H. Zhang, et al., Probing the nature of upconversion nanocrystals: instrumentation matters, Chem. Soc. Rev. 44 (2015) 1479−1508.
[26] Y. Yang, C. Liu, P. Mao, L. Wang, Upconversion luminescence and photodegradation performances of Pr doped Y2SiO5 nanomaterials, J. Nanomater. 2013 (2013) 427370.

[27] E.L. Cates, M. Cho, J. Kim, Converting visible light into UVC: microbial inactivation by Pr3+-activated upconversion materials, Environ. Sci. Technol. 45 (2011) 3680−3686.
[28] W. Gao, W.Y. Zhang, G.X. Lu, A two-pronged strategy to enhance visible-light-driven overall water splitting via visible-to-ultraviolet upconversion coupling with hydrogen-oxygen recombination inhibition, Appl. Catal. B Environ. 212 (2017) 23−31.
[29] W. Gao, W.Y. Zhang, B. Tian, et al., Visible light driven water splitting over $CaTiO_3/Pr^{3+}$-Y_2SiO_5/RGO catalyst in reactor equipped artificial gill, Appl. Catal. B Environ. 224 (2018) 553−562.
[30] G.X. Lu, B. Tian, Formation of deuterium and helium during photocatalytic hydrogen generation from water catalyzed by Pt-graphene sensitized with Br-dye under visible light irradiation, J. Mol. Catal. 31 (2017) 101−104.
[31] G.X. Lu, W.L. Zhen, Formation of helium-3 and helium-4 during photocatalytic hydrogen generation over cadmium sulfide under visible light irradiation, J. Mol. Catal. 31 (2017) 299−304.
[32] G.X. Lu, W.Y. Zhang, Photocatalytic hydrogen evolution and induced transmutation of potassium to calcium via low-energy nuclear reaction (LENR) driven by visible light, J. Mol. Catal. 31 (2017) 401−410.
[33] G.X. Lu, X.Q. Zhang, W.L. Zhen, The detection of K-Ca transmutation in the mixture of K and hydride chemicals, J. Mol. Catal. 33 (2019) 1−9.

Further reading

[1] H. Yuan, X. Wang, B. Lian, et al., Generation and electric control of spin-valley-coupled circular photogalvanic current in WSe2, Nat. Nanotechnol. 9 (2014) 851−857.
[2] V. Kiran, S.P. Mathew, S.R. Cohen, et al., Helicenes-a new class of organic spin filter, Adv. Mater. 28 (2016) 1957−1962.

This page intentionally left blank

Recent advances in the development of photocatalytic NOx abatement

14

Van-Huy Nguyen[1], *Joseph Che-Chin Yu*[2], *Chao-Wei Huang*[3], *Jeffrey C.-S. Wu*[2]
[1]Institute of Research and Development, Duy Tan University, Da Nang, Vietnam;
[2]Department of Chemical Engineering, National Taiwan University, Taipei, Taiwan;
[3]Department of Chemical and Materials Engineering, National Kaohsiung University of Science and Technology, Kaohsiung, Taiwan

1. Introduction

Nowadays, improving air quality has become a globally urgent issue. The emission of nitrogen oxides (NOx) family that include nitric oxide (NO), nitrogen monoxide (NO), nitrogen dioxide (NO_2), nitrous oxide (N_2O), and their derivatives belongs to tropospheric air pollutants and has a wide range of human health, environment, and biological ecosystem impacts [1].

In the past three decades, the research in the field of NOx abatement, including NO oxidation, NO decomposition, and NO selective catalytic reduction (SCR) by reducing agents (carbon monoxide (CO), hydrogen (H_2), ammonia (NH_3), hydrocarbons (HC)), has grown significantly. Over the decades, the SCR has been developed and applied widely in industry, remained the mainstream approach to eliminating NOx. To reach the working temperature that is required by SCR, an SCR system is usually installed in front of cyclone dust collectors and desulfurization systems. However, SCR components are also installed elsewhere to prevent catalysts from poisoning particles and sulfur compounds. In such arrangements, flue gas will not be sufficiently hot to preheat an SCR system, so additional heating equipment should be incorporated.

Recently, photocatalysis technology, which could effectively work under low reaction temperature and efficiently reduce energy consumption, becomes a promising approach for NOx abatement [2]. Generally, the photocatalytic NOx abatement mainly includes three different routes: photooxidation, photodecomposition, and photo-SCR. For the photooxidation of NOx, this method transforms NOx into NO_2, nitrates NO_3^- that need to be washed from the surface of the photocatalyst. Photo-SCR and photodecomposition, which are belonged to reduction methods, convert NO into N_2 and other harmless gaseous compounds. The photo-NOx abatement offers many advantages, these include (a) excellent N_2 selectivity with considerable NOx conversion at ambient temperatures and pressures, (b) cost-effective, (c) environmental energy harvesting based on solar light, (d) energy saving, no extra heat required, (e) no extra reactants required, and (f) NOx recovered as nitrates NO_3^-, which is a conceivable raw material for fertilizers [2].

Current Developments in Photocatalysis and Photocatalytic Materials
https://doi.org/10.1016/B978-0-12-819000-5.00014-X

In this chapter, primary attention is given on discussing the progress and development of photocatalytic NOx abatement, including photocatalysts, their photocatalytic performance, photoreactor, and photomechanism. The overall conclusion is drawn with the potential future research direction in the development of photo-deNOx.

2. Tailoring the photocatalysts for photocatalytic NOx abatement

Although there has been extensive research on photo-NOx abatement, its photocatalytic efficiency is still needed to be further enhanced. Because the activity of a simple photocatalyst is early determined, then the first step is to modify its photocatalyst.

2.1 Photocatalysts for photooxidation of NOx

Titanium dioxide (TiO_2) is a highly studied semiconductor due to its nontoxicity, chemical stability, wide availability, nonexpensive, structural, and electronic properties [3]. At present, titania-based photocatalysts, among candidates, have also received the most attention included TiO_2, ultrafine TiO_2 particles, Pd-modified TiO_2 (PdO/TiO_2, Pd/TiO_2), TiO_2/MCM-41, TiO_2 loading on woven glass fabric, TiO_2 coatings containing aluminum particles, TiO_2 nanoparticles incorporated in a polymer matrix—based coating, and TiO_2 coatings elaborated by various thermal spraying methods. However, it is noted that titania has a removal efficiency insufficient for practical use. On light irradiation of TiO_2 in the air or O_2 and N_2 mixtures polluted with NO, the formation of NO_2 could partly adsorb on the surface of TiO_2 then block the active sites of its surface, resulting in shortening its lifetime [4].

To solve the above issue, there have been many studies on improvement of its activity by dispersing TiO_2 on the supports with a high adsorption capacity. For example, TiO_2 zeolite composites, TiO_2 dispersed over alumina support (TiO_2/Al_2O_3), TiO_2 immobilized on activated carbon filter (TiO_2/AC), a composite TiO_2—metal compound (MC) sheet with the MCs were used such as CaO, MgO, $CaCO_3$, Al_2O_3, Fe_2O_3, and TiO_2-AC-Fe_2O_3. As expected, the combination of photocatalyst TiO_2 with adsorbents appears to have higher photocatalytic efficiency. The above studies, however, are mostly conducted under UV light irradiation. Therefore, there is a need for developing the photocatalysts that could shift the absorption edge to longer wavelength ($\lambda > 400$ nm).

Doping of titania with metals/metal oxides has been proposed; these include Pt/TiO_2, Sn/TiO_2, Rh/TiO_2, Mn/TiO_2, and transition metal—loaded M (Cu, V, and Cr)/TiO_2. However, the drawback of this method is the metal ions/metal oxides dopant might act as recombination centers of e^- and h^+ [5]. Hence, extensive study has been conducted on the development of the anion-doped TiO_2, such as N-doped TiO_2, C-doped TiO_2, B, N-codoped TiO_2, Fe-loaded N-doped TiO_2, and Pt-loaded N-doped TiO_2. On another approach, the method to modify the surface of powder

materials by a low-temperature plasma treatment is also received considerable attention, including the hydrogen plasma−treated TiO_2 powders.

The following focus of photocatalysts for photocatalytic oxidation of NOx is active to improve the photocatalytic efficiency, lifetime, and visible light−responsive behavior of photocatalysts. Although the efficiency in photooxidation of NOx is desirable, this technique does not close to the targets set for practical use. The reason is that photooxidation would transform NO into HNO_3 via the formation of HNO_2 and NO_2 which bring some disadvantages for this process, such as (a) higher toxicity and stability of NO_2 than that of NO and (b) the formation of nitrates NO_3^- on photocatalyst surface that requires consistent catalyst regeneration.

2.2 Photocatalysts for photodecomposition of NOx

Various photocatalysts, such as TiO_2, Ti/Y-zeolite, Ti/ZSM-5, Ti/HMS, Ti/MCM-41, Cu^+/SiO_2, Cr/TiO_2, V/TiO_2, Ag/TiO_2, Cu^+/ZSM-5 zeolites, and Ag^+/ZSM-5 zeolites, have been developed efficiently to function with UV and visible light for the photocatalytic decomposition of NOx. It notes that the photodecomposition of NO is found to strongly depend on the local structure of the incorporating transition metal ions (Ti, V, Cr, Cu, Ag, Mg) [6]. Firstly, the implanted metal ions only modify the electronic property of the photocatalyst to enable the absorption of visible light and do not work as the electron−hole recombination center. Second, the highly dispersed isolated metal ions play a vital role in the initiation of the photodecomposition of NO into N and O. To the best of our knowledge, photodecomposition is an ideal process. However, it has not yet been investigated in the presence of other compounds, especially O_2 and H_2O, which typically pose problems for the photocatalytic reactivity.

2.3 Photocatalysts for photo-SCR of NOx

Using photoenergy as the driving force, photo-SCR of NOx is desirable for energy-saving purposes. It occurs on a photocatalyst surface under light irradiation and involves the reduction of NOx with the reducing agents, such as NH_3, CO, or hydrocarbons. Without these sacrificed reductants, the selectivity toward the formation of NO_2, a more toxic type of NOx as compared with NO, could be occurred [7].

2.3.1 Photocatalysts of photo-SCR with NH_3

Much research has been done over titania-based photocatalysts for photo-SCR with NH_3-reducing agent (NH_3/photo-SCR), these include TiO_2, pressed wafers of TiO_2, TiO_2 nanotube arrays, WO_3/TiO_2, Si/TiO_2, MnO_2-(Co_3O_4)/TiO_2, and transition metal (V, Cr, Mn, Fe, Co, Ni, Cu, Zn, Y, Zr, Nb, Mo, Ta, or W) oxide−modified TiO_2. Among various titania-based photocatalysts, WO_3/TiO_2 shows the best photo-deNOx activity at the gas hourly space velocity (GHSV) of 16,000 h^{-1} (as shown in Fig. 14.1), which might be only sufficient in typical stationary sources such as power plants, blast furnaces, and incinerators. However, a very high GHSV value

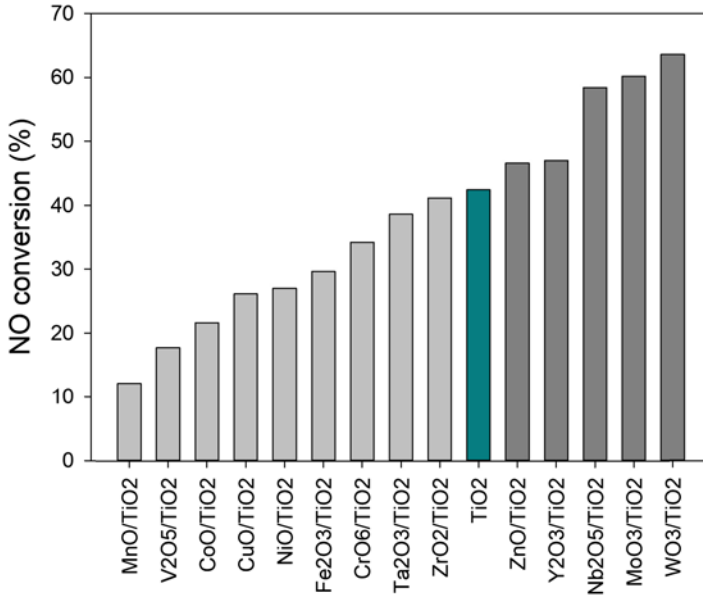

Figure 14.1 The conversion of NO in the photo-SCR with NH_3 over various metal oxide transition metal oxides (1.0 wt%) to modify TiO_2 photocatalysts. Reaction conditions: NO, 1000 ppm; NH_3, 1000 ppm; O_2, 2%; Ar balance; GHSV = 50,000 h^{-1}.
Data was collected from Yamazoe et al. Research on Chemical Intermediates, 34 (2008) 487−494.

(approximately 100,000 h^{-1}) is required in diesel engines owing to the limited installation space of the photo-deNOx process and a high flow rate of the exhaust gas [8].

Extension of the absorption wavelength to the visible light region is an effective way to improve the photocatalytic activity by dye-sensitizer, included TCPP (tetra(*p*-carboxyphenyl)porphyrin) and Ru(2,2′-bipyridyl-4,4′-dicarboxylic acid)$_2$(NCS)$_2$ complex (N3-dye). Among 15 different dyes modified TiO_2, Ru(2,2′-bipyridyl-4,4′-dicarboxylic acid)$_2$(NCS)$_2$ complex (N3-dye) could achieve the best performance (NO conversion >99%, N_2 selectivity >99%) at a high GHSV of 100,000 h^{-1} after 30min of visible light irradiation ($\lambda > 400$ nm) [9].

In another approach, composite mixed oxides, especially perovskite-type photocatalysts, have also considered as a group of promising catalysts for photo-SCR as they are at a lower price, mixed valence states of the transition metals, and higher stability. Many efforts are undergoing to study and propose some promising candidates with excellent performances, such as $LaFe_{04}Mn_{0.6}O_3$/attapulgite (ATP), nitrogen-doped carbon quantum dots (N-CQDs)-modified $PrFeO_3$/palygorskite (Pal), $LaFe_{0.5}Ni_{0.5}O_3$/Pal, and $Pr_{1-x}Ce_xFeO_3$/Pal. Interestingly, $Pr_{0.7}Ce_{0.3}FeO_3$/Pal performs an excellent catalytic activity (the NO conversion achieves 92%, and N_2 selectivity reaches nearly 99%) at a high GHSV of 50,000 h^{-1} with a remarkable resistance to SO_2 and H_2O poisoning [10]. Together with the dye-sensitized photocatalysts,

perovskite-type photocatalysts are expected to open up new windows for industrial denitrification applications.

2.3.2 Photocatalysts of photo-SCR with CO

Although NH_3-reducing agent can effectively reduce NO under light irradiation, a risk of ammonia leakage and its corrosive nature make it unfavorable for environmental applications. It is well known that CO is one of the main toxic gaseous pollutants emanating from an automobile exhaust that requires prevention and control measures [11]. To deal with the above issues, an ideal route to eliminate these pollutants simultaneously is through photo-SCR with CO as a reducing agent (CO/photo-SCR). However, it is noted that most developed photocatalysts efficiently function with only UV light; these include TiO_2, Ru/TiO_2, Rh/TiO_2, and Cu/TiO_2, 1% Pd/TiO_2 and $Ti_{1-x}Pd_xO_{2-\delta}$ (where $x = 0.05-0.3$), $Ag-TiO_2$, Ru/TiO_2, single-site photocatalysts: M/SiO_2 (M = Mo, V, and Cr), and MoO_3/SiO_2.

2.3.3 Photocatalysts of photo-SCR with hydrocarbons

As a potential alternative without those drawbacks inherent in the NH_3/photo-SCR, the photo-SCR with hydrocarbons (HC/photo-SCR) also offers many advantages, such as a convenient and inexpensive process due to the presence of unburned hydrocarbons in the exhaust gas. There has been an intensive study on many hydrocarbons for the HC/photo-SCR, such as CH_4, C_2H_4, C_2H_6, C_3H_6, C_3H_8, and C_4H_{10}. However, it is noted that although hydrocarbons are relatively easy to handle as reductants in photocatalytic deNOx, their performance still has much room for improvement. Many studies have been focused on developing efficient photocatalysts. Among several metals and supporting materials, titania-based photocatalysts had received the most attention; these include TiO_2, TiO_2 nanosheets, Pd/TiO_2, PdO/TiO_2, Pt/TiO_2, $PtOxPdOy/TiO_2$, and TiO_2-coated α-Al_2O_3/γ-Al_2O_3. There have been very few studies that work on non-TiO_2 based, such as vanadium silicalite-1 (VS-1, Si/V = 120).

3. Designing of photoreactors for photocatalytic NOx abatement

In addition to the photocatalyst, different photoreactor types would affect the photocatalytic efficiency, such as the phases involved (single phase, multiphase), the mode of hydrodynamic operation (batch, semibatch, or continuous), the mixing and flow characteristics, the shape geometric configuration, and the light source specifications [12]. There are several photocatalytic reactors that could be used for photo-deNOx. However, to choose the right configurations, photoreactor types play an important role and could affect the efficiency of photocatalysis process.

In most studies, the photodecomposition of NO is conducted under closed reaction systems. For the first time, Zhang et al. compares the flow and closed reaction systems [13]. It is found that photocatalysts are desirable for effective and efficient

decomposition of NO into N_2 and O_2 under a flow reaction system, even for prolonged irradiation periods. Further studies have focused on the flow reaction system. Lim et al. propose a modified two-dimensional fluidized-bed photoreactor, which has efficient contact between the photocatalyst and reactant gas with a good transmission of UV light and, consequently, increases in NO decomposition efficiency compared with the annular flow-type photoreactor [14]. For photo-SCR, Poulston et al. developed the continuous small photoreactor [15]. Yu et al. coated photocatalyst on optical fibers and used in a continuous flow optical fiber photoreactor [16]. This design could provide effectively light irradiation on the photocatalyst through the optical fiber, and as a consequent, the efficiency of photoreaction could be enhanced. Yu et al. also proposed a novel design that to insert optical fibers into every monolith channels, named a photocatalyst-coated monolith photoreactor, in which the monolith channels could be adequately illuminated, thus improving the efficiency of photoreaction [17].

Despite the low photoefficiency, the approach to develop a new and optimize the current photocatalytic systems, including photocatalyst and photoreactor, is also essential and necessary for further studies.

4. Elucidating of reaction pathways for photocatalytic NOx abatement

For broad applicability, it is necessary to understand the reaction pathways and the mechanisms of the photoreaction. Hence, this section will focus on reviewing the reaction pathways for the photocatalytic NOx abatement.

4.1 Reaction pathways of photooxidation

The reaction pathways of NO photooxidation over photocatalysts might undergo many states (Scheme 14.1). For the typical photocatalytic reactions, the generation of election−hole (e^-, h^+) pairs, hydroxyl (•OH), and oxygen ($O_2^{\bullet-}$) radicals on the photocatalyst surface plays an important role. The reaction pathways of photooxidation of NO to NO_3^- via NO_2 (intermediate) have been confirmed previously [18]. It is worthy

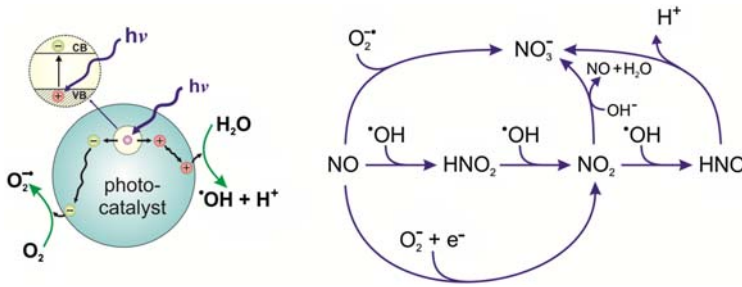

Scheme 14.1 The reaction pathways of NO photooxidation over photocatalysts.

of note that the photooxidation efficiency of NO depends strongly on the presence of water in the reaction [19], as a high concentration of relative humidity contributes to the transformation of NO_2 into HNO_3.

4.2 Reaction pathways of photodecomposition

As mentioned previously, the generation of election−hole (e^-, h^+) pairs on the photocatalyst surface plays a crucial role in this photoreaction. Scheme 14.2 represents the possible reaction pathways occurring during the photocatalytic decomposition of NO on the surface of TiO_2 photocatalyst. Under light irradiation, the electron transfer occurs from the electron trapped centers into the antibonding orbitals of adsorbed NO molecules, resulting in their decomposition and formation of $N_{(ads)}$ and $O_{(ads)}$ surface species [20]. Then, above species would migrate on the TiO_2 surface and react with other surface species (e.g., $NO_{(ads)}$, $N_{(ads)}$, $O_{(ads)}$ forming products such as $N_2O_{(gas)}$, $NO_{2(ads)}$, $O_{2(gas)}$ and $N_{2(gas)}$). It is noted that the primary reaction is $NO_{(ads)} + N_{(ads)} \rightarrow N_2O_{(ads)}$, which generates N_2O as the major product [21]. On the other hand, the mechanism of photodecomposition of $NO_{(ads)}$ to $N_{(ads)} + O_{(ads)}$ via $NO^-{}_{(ads)}$ (intermediate) is also proposed [22].

4.3 Reaction pathways of photo-SCR

Besides the efforts to enhance the photocatalytic efficiency, much attention has been paid to clarify the reaction pathways behind this reaction. In this section, the mechanisms of photo-SCR are reviewed based on different types of reducing agent and photocatalyst. Firstly, the reaction pathways of the photo-SCR with NH_3 over TiO_2 are proposed using spectroscopic [23], kinetic [24], and theoretical [25] methods, as shown in Scheme 14.3 [26]. Theoretical and experimental studies consistently show that NH_3 is adsorbed firstly on a Lewis acid site of TiO_2. Then the photoactivation of NH_3 adsorbed on TiO_2 to generate $\cdot NH_2$ radical occurs through two pathways: (1) the photoexcitation of TiO_2 under UV light irradiation (<400 nm) and (2) the direct

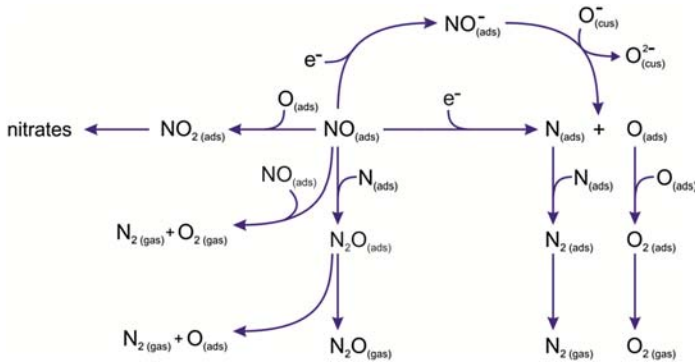

Scheme 14.2 The reaction pathways of NO photodecomposition over photocatalysts.

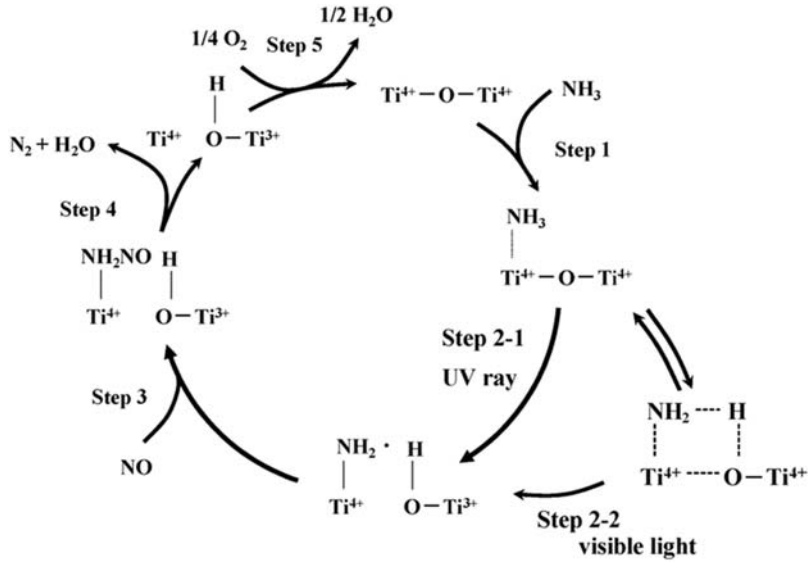

Scheme 14.3 The reaction pathways of the photo-SCR with NH_3 under UV/visible light irradiation over TiO_2.
Reprinted from S. Yamazoe et al./Applied Catalysis B: Environmental 83 (2008) 123−130.

electron transfer from N2p of adsorbed NH_3 to Ti3d that enabling the photo-SCR to proceed under visible light (400−450 nm) irradiation. Following, the $\cdot NH_2$ radical reacts with NO to form nitrosoamide (NH_2NO) intermediate species. Then the NH_2NO intermediate species is further decomposed to N_2 and H_2O. For the active site, the Ti^{3+} species of TiO_2, which is reduced by H_2, is reoxidized to the Ti^{4+} species.

In the previous study, the reaction pathways of the photo-SCR with NH_3 over dye-sensitized photocatalyst (Ru(2,2′-bipyridyl-4,4′-dicarboxylic acid)$_2$(NCS)$_2$ complex (N3-dye)-modified TiO_2) is successfully proposed [9]. Firstly, NO and NH_3 are adsorbed on the catalyst surface. Following, the electron injection from photoexcited Ru dyes into the conduction band of TiO_2. Then the activation of NH_3 happened by oxidized Ru dyes to generate the $\cdot NH_2$ radical. After that, the $\cdot NH_2$ radical would react with NO_2^- to form N_2 and H_2O. For the active site, the Ti^{3+} species of TiO_2 is reoxidized to the Ti^{4+} species by O_2.

Scheme 14.4 reveals the reaction pathways of the photo-SCR with NH_3 over perovskite-type photocatalyst ($LaFe_{1-x}Mn_xO_3$/ATP) [27]. Similar to the mechanism over TiO_2, NH_3 is adsorbed on Lewis acid site of $LaFe_{1-x}Mn_xO_3$. Both of $LaFe_{1-x}Mn_xO_3$ and $LaMnO_3$ are excited under visible light where photogenerated electrons on the conduction band of $LaMnO_3$ directly transfer to the conduction band of $LaFe_{1-x}Mn_xO_3$, which hinders the recombination of electron−hole pairs. Subsequently, the photogenerated electrons coming from $LaMnO_3$ and remained in the conduction band of $LaFe_{1-x}Mn_xO_3$ reduce Fe^{3+} to Fe^{2+}. On the other side, the holes in the valence band of $LaMnO_3$ transfer to the valence band of $LaFe_{1-x}Mn_xO_3$, which

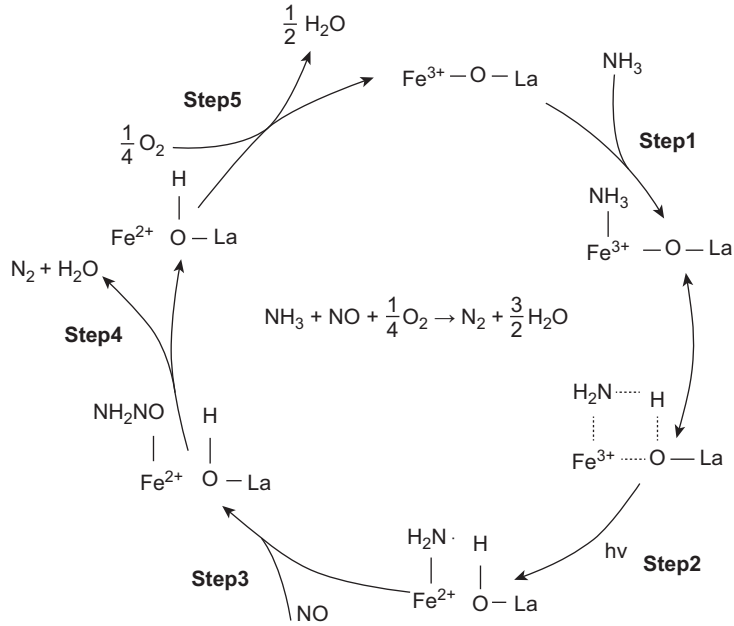

Scheme 14.4 The reaction pathways of the photo-SCR with NH_3 under visible light irradiation over by $LaFe_{1-x}MnxO_3$/ATP photocatalyst.
Reprinted from Li et al. Chemical Engineering Journal, 320 (2017) 211−221.

lead to forming more photogenerated holes which are captured by the $\cdot NH_2$ species developed from NH_3 adsorbed on the surface of $LaFe_{1-x}Mn_xO_3$ to produce $\cdot NH_2$ radical. Then $\cdot NH_2$ radical is attacked by NO and produces NH_2NO intermediate species. After that, the unstable intermediate NH_2NO is decomposed into N_2 and H_2O quickly. Finally, Fe^{2+} is reoxidized to Fe^{3+} by adsorbed O_2.

For the photo-SCR with CO, the possible reactions occurring on the surface of TiO_2 photocatalyst might be represented as follows [21]:

$$TiO_2 + h\nu \rightarrow e^- + h^+ \quad (1)$$

$$NO_{(ads)} + e^- \rightarrow N_{(ads)} + O_{(ads)} \quad (2)$$

$$O_{(ads)} + CO_{(ads)} \rightarrow CO_{2(gas)} \quad (3)$$

$$2NO_{(ads)} + CO_{(ads)} \rightarrow N_2O_{(ads)} + CO_{2(ads)} \quad (4)$$

$$N_2O_{(ads)} + CO_{(ads)} \rightarrow N_{2(gas)} + CO_{2(ads)} \quad (5)$$

$$N_{(ads)} + N_{(ads)} \rightarrow N_{2(ads)} \quad (6)$$

$$N_{2(ads)} \rightarrow N_{2(gas)} \quad (7)$$

$$N_2O_{(ads)} \rightarrow N_2O_{(gas)} \quad (8)$$

$$CO_{2(ads)} \rightarrow CO_{2(gas)} \quad (9)$$

With the presence of CO, it would be beneficial for the efficiency of photo-SCR. Under UV light irradiation, CO could help for the formation of N_2O or act as a scavenger for N_2O to produce N_2 and CO_2. On another approach, an in situ FTIR study is conducted to reveal the reaction mechanism of photo-SCR with CO over three single-site photocatalysts: Mo/SiO_2, V/SiO_2, and Cr/SiO_2, as illustrated in Scheme 14.5 [28]. Among three single-site photocatalysts, Mo/SiO_2 exhibits a high photoactivity, leading to the production of both N_2 and CO_2. Contrarily, NO is only photoreduced into N_2O over V/SiO_2. The reason might come from the fact that the formation of unreactive NO−adsorbed V^{3+} oxide species is very stable and could prohibit the reoxidation of V^{3+} oxide species by N_2O. On the other hand, Cr/SiO_2 does not promote photo-SCR. The reoxidation to produce the original Cr^{6+} species hardly occurs due to the stability of unreactive NO−adsorbed Cr^{2+} oxide species.

For the photo-SCR with HC, their reaction pathways are still poorly understood. Wu et al. use in situ FTIR spectroscopy to study the photoreaction process in the presence of CH_4 over TiO_2-supported photocatalyst [29]. There is a variety of photoreaction intermediates that have been observed in the IR spectra. Before the light is turned on, NO is adsorbed on the surface of the catalyst and converted into bidentate nitrite and monodentate nitrate while CH_4 is adsorbed to form (CH_3^-). During UV light irradiation, monodentate nitrites and (CH_3^-) were oxidized to monodentate and bidentate nitrates, formic acid, and methanol by superoxo species. Possible reaction pathways of photo-SCR with CH_4 are proposed based on the basis of the intermediates and products generated on the surface of the photocatalysts (Scheme 14.6) [29].

4.4 Reaction pathways for photo and thermal catalytic removal of flue gas

Although numerous studies have been focused on photocatalytic removal of NO, there is little information available on the mechanism for photoremoval of NO in the flue gas. In the previous study, three types of co-feeds, including NO with O_2+H_2O, NO with C_4H_{10}, and NO with C_4H_{10} and O_2+H_2O to simulate the flue gas, are investigated at the different reaction temperature (40−300°C) [30]. Based on our knowledge of the species obtaining during the photoreaction and the change in the thermodynamic properties of reactions, possible reaction pathways of photo and thermal catalytic removal of NO in flue gas over TiO_2 is proposed systematically in Scheme 14.7.

There might exist three types of photocatalytic reaction, including photooxidation, photodecomposition, and photo-SCR, during the photocatalytic removal of NO in the flue gas based on the reaction temperature. From a thermodynamic perspective, the values for the changes of Gibbs free energies of the formation of products are

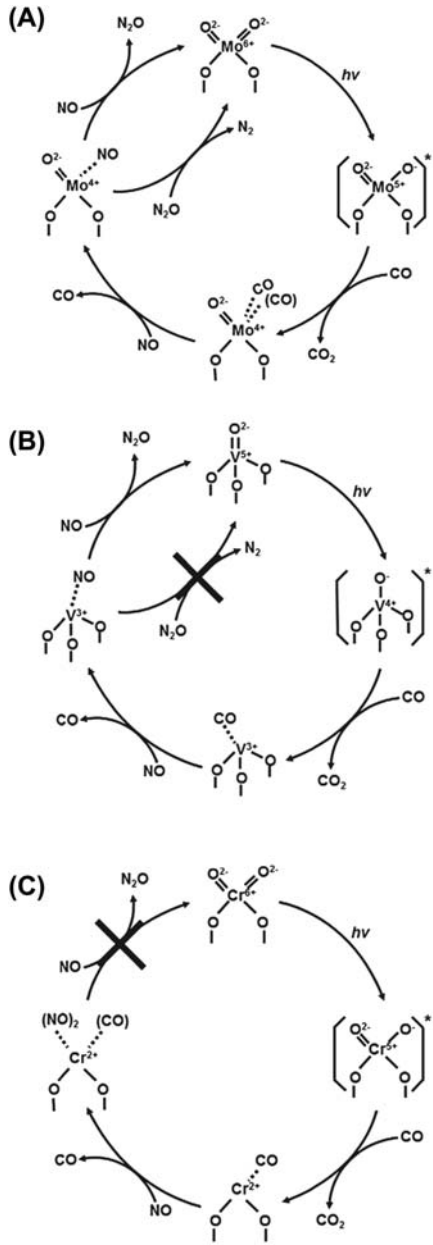

Scheme 14.5 The reaction pathways of the photo-SCR with CO under UV light irradiation over by (A) Mo/SiO_2, (B) V/SiO_2, and (C) Cr/SiO_2 photocatalysts.
Reprinted from T. Toyao et al. Journal of Catalysis 299 (2013) 232−239.

Current Developments in Photocatalysis and Photocatalytic Materials

New Horizons in Photocatalysis

Reviews the fundamental chemistry and latest progress in the development of organic and inorganic materials for use in photocatalysis.

Edited by

Xinchen Wang
Dean of the College of Chemistry and Director of the State Key Laboratory of Photocatalysis on Energy and Environment, Fuzhou University, Fuzhou, P. R. China

Masakazu Anpo
Special Honor Professor and International Advisor, State Key Laboratory of Photocatalysis on Energy and Environment, Fuzhou University, Fuzhou, P. R. China; Emeritus Professor, Osaka Prefecture University, Osaka, Japan

Xianzhi Fu
President, Fuzhou University, Fuzhou, P. R. China

Photocatalytic materials can improve the efficiency and sustainability of processes and offer novel ways to address issues across a wide range of fields—from sustainable chemistry and energy production to environmental remediation. *Current Developments in Photocatalysis and Photocatalytic Materials* provides an overview of the latest advances in this field, offering insight into the chemistry and activity of the latest generation of photocatalytic materials.

After an introduction to photocatalysis and photocatalytic materials, this book goes on to outline a wide selection of photocatalytic materials, not only covering typical metal oxide photocatalysts such as TiO2 but also exploring newly developed organic semiconducting photocatalysts, such as g-C_3N_4.

Drawing on the experience of an expert team of contributors, *Current Developments in Photocatalysis and Photocatalytic Materials* highlights the new horizons of photocatalysis, in which photocatalytic materials will come to play an important role in our day-to-day lives.

Key Features

- Reviews developments in both organic- and inorganic-based materials for use in photocatalysis
- Presents the fundamental chemistry and activity of a broad range of key photocatalytic materials, including both typical and novel materials
- Highlights the role photocatalytic materials can play in sustainable applications

ISBN 978-0-12-819000-5

9 780128 190005

ELSEVIER elsevier.com/books-and-journals